JOURNAL OF MATERIALS SCIENCE 27 (1992) 5343–5347

Effect of rare-earth treatment on the banded microstructure and fracture properties of a 16 Mn steel

LONGQUAN SHI, D. O. NORTHWOOD
Engineering Materials Group, Department of Mechanical Engineering, University of Windsor, Windsor, Ontario, Canada N9B 3P4

The two treatments, namely rare-earth (RE) additions to the mould and Ca–Si injection into the ladle, were used to control the MnS inclusion shape in a 16 Mn steel. The critical crack opening displacement, δ_c, method and tensile testing were used to determine the fracture properties of the steel sheets. Scanning electron microscope (SEM) fractography of the fracture surface of tensile specimens tested at room temperature clearly showed the banded structure of the steel sheets in all, even modified, steels. The RE treatment improved the fracture properties both by sulphide inclusion shape control and by reducing microstructural heterogeneity.

1. Introduction

The amount, size, shape and distribution of inclusions in steels can greatly affect their mechanical properties [1]. A plain carbon steel, such as 16 Mn steel (similar to AISI 1020 with respect to its chemical composition), which contains a small amount of sulphur, will form a "Type II" sulphide inclusion structure [2]. This structure results from the formation of MnS–Fe eutectic at the as-cast grain boundaries, due to the very low solubility of sulphur in the solid steel – less than 0.001% S in the b c c structure [3]. This "Type II" structure weakens the as-cast structure and also results in elongated MnS inclusions in the hot-rolled steel products [4].

A calcium treatment can be used to reduce the sulphur content to a very low level, about 0.008 wt %, but cannot remove all the MnS inclusions from the steel [4]. However, this inclusion control can be obtained by use of a rare-earth (RE) treatment. Provided the RE/S ratio is larger than about 3 then complete inclusion shape control can be achieved [4]. Also, the RE addition leads to a more homogeneous distribution of manganese in the banded (pearlite–ferrite) structure formed in hot-rolled sheet [4]. In this study, the effects of a RE treatment on the fracture properties of 16 Mn steel were determined, and the results examined in the light of fractographic and microstructural observations [4, 5].

2. Experimental procedure

2.1. Materials

The specimens used in this experiment were all taken from the centre of the as-rolled steel sheets. The chemical composition at the mid-point of the ingots was as follows: 0.19% C, 1.4% Mn, 0.41% Si, 0.023% P (all composition in wt %). The 16 Mn steel was refined in a 300 ton open-hearth furnace. A two-ladle system was used: Ladle A had no Ca–Si injected and Ladle B was injected with 3.4 kg Ca–Si per ton steel. The steel from these ladles was poured into moulds with different RE contents (see Table I). The flat ingots which each weighed 12.5 ton were hot rolled into the sheet, 6 mm thick and 1100 mm wide.

2.2. Methods

The critical crack opening displacement (COD), δ_c, measurements were made on the three-point bend specimens, with length 50 mm, width 10 mm, and thickness 5 mm. The bend gauge length was 40 mm. The specimens had a 3 mm machined notch and a 2 mm preset fatigue crack (the fatigue crack was produced on a 400 kg high-frequency fatigue test machine using loads $P_{f_{max}} = 140$ kg and $P_{f_{min}} = 20$ kg). The test procedure and the data processing followed the National Standard of the People's Republic of China (PRC GB 2358-80). The material constants used for the calculation were as follows: Young's modulus, E, 206 GPa; yield strength, σ_y, 425 MPa; Poisson's ratio, ν, 0.30; plastic zone correction factor, r_p, 0.45. In order to avoid any (crack) size change due to plastic deformation, following the three-point bend tests the specimens were then broken by a second fatigue cracking, prior to the bending crack extension length, Δa, measurement being made. A blueing treatment of 300 °C for 1 h was used on all of the bend specimens prior to second fatigue cracking in order to delineate the crack due to bending from the preset fatigue crack and the second fatigue crack.

The tensile specimens for the room-temperature tensile tests and hardness tests were taken from the L (rolling) direction in the steel sheet. They all had a diameter of 5 mm and a gauge length of 10 mm. The

0022–2461

TABLE I Treatment methods for steels

Number of steel ingot	Ladle number	Ca–Si treatment in ladle (kg Ca–Si/ton steel)	RE addition to mould (wt %)
6	A	–	–
5	A	–	0.1
4	B	3.4	–
3	B	3.4	0.03
2	B	3.4	0.06
1	B	3.4	0.1

TABLE II Results of the COD tests

Ingot number	δ_c Values (mm)	
	Rolling direction	Transverse direction
6	0.15	0.086
5	0.15	0.15
4	0.15	0.10
3	0.15	0.15
2	0.15	0.15
1	0.15	0.15

test was done on a conventional tensile testing machine. The speed of the crosshead during tensile test was 0.02 mm s^{-1} The hardness test was made on the polished surface parallel to the steel sheet surface. This test was conducted with a 10 mm diameter steel ball at a load of 3000 kg.

The low magnification optical fractography of the COD fracture surface was made to show the typical crack pattern in the COD test specimens. It also provided a macroscale information on the fracture pattern of the steel (from the bending fracture surface); e.g. the tearing crack between the banded structures.

SEM observation of the tensile fracture surface was made on a set of samples with the six different treatments. The aim was to determine the effect of the RE treatment on the ductile fracture pattern of the steel. This method was also used to examine the inclusions, especially the elongated MnS inclusions present in the banded structure and how they respond to the ductile tensile fracture. These inclusions are usually found at the interface between the proeutectoid ferrite and the pearlite in the banded microstructure.

3. Results

3.1. Mechanical properties

The COD test results are listed in Table II. From Table II it can be seen that the RE treatment eliminates the anisotropy in δ_c values between the rolling and the transverse directions. All the δ_c values are approximately 0.15 mm in the rolling direction, regardless of their treatment. However, for the untreated sample (Sample 6), δ_c was only 0.086 mm in transverse direction, and for the sample with only a calcium treatment (Sample 4), δ_c was 0.10 mm in transverse direction. The δ_c value for all the samples with a RE treatment (Samples 5, 3, 2, 1) was 0.15 mm, i.e. the same as in the rolling direction. This was due to the RE treatment which completely modified the shape of the inclusions in the steel. As was shown in a previous work, all the samples with an RE treatment had no elongated MnS inclusions [4], which will cause a stress concentration when the specimens were subject to a plastic strain and initiate a microcrack, thereby decrease the δ_c value. A RE inclusion shape control will modify MnS inclusion to spherical RE sulphide inclusions and reduce the stress concentration arising from the shape of the inclusions present in the steel.

The tensile test and hardness test results are given in Table III. These tests show that all six treatment specimens had the same room-temperature tensile properties such as tensile strength, σ_t, yield strength, $\sigma_{0.2}$, elongation percentage, δ, and percentage reduction of area, ψ, as well as Brinell hardness, HB. Note that all the specimens for these tests were taken from the rolling direction. And, as such, the tensile properties and hardness are not affected by the elongated MnS inclusions because of their orientation. The difference in the values for the different treatments were within 10% of each other in the tests. Table III also gives the average values of all the tests made on all six different treatments.

3.2. Low-magnification fractography of the COD test samples and SEM fractography of the tensile specimen

A set of low-magnification optical fractographs of the COD test samples is given in Fig. 1a and b. In Fig. 1a, the upper row are the samples from ingots 6, 5, 4, 3, 2, respectively, going from left to right; the lower row are all samples from ingot 1. Similarly in Fig. 1b, the upper row are the samples from ingot 6, 5, 4, 3, 2, respectively, going from left to right, the lower row are all samples from ingot 1, but the crack extensions, Δa,

TABLE III The tensile properties of as-rolled 16 Mn steel

Ingot	Tensile strength, σ_t (MPa)	Yield strength, σ_y (MPa)	Brinell hardness, HB	Elongation, δ (%)	Reduction of area, ψ (%)
6	441.2	329.8	145.4	35.2	56.8
5	460.3	344.3	148.8	36.2	58.5
4	454.5	341.7	150.5	32.8	60.3
3	460.8	338.6	143.9	34.6	59.7
2	440.0	327.1	140.2	34.2	55.6
1	443.3	331.4	141.0	33.9	57.2
Average	450.0	335.5	145.0	34.5	58.0

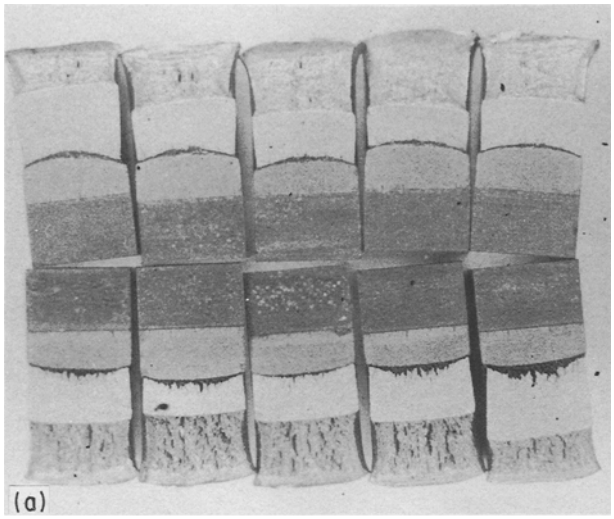

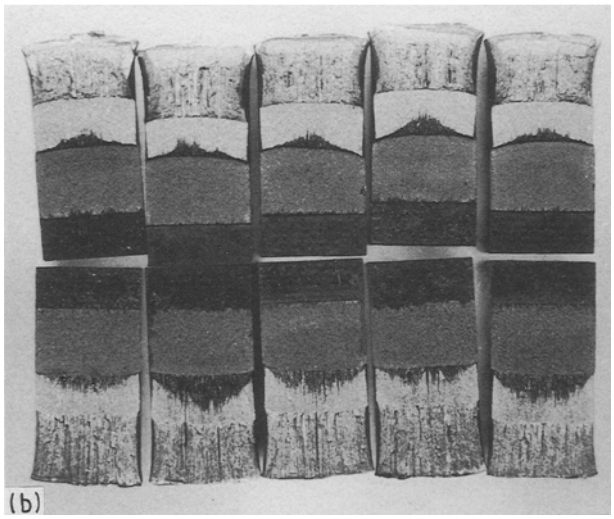

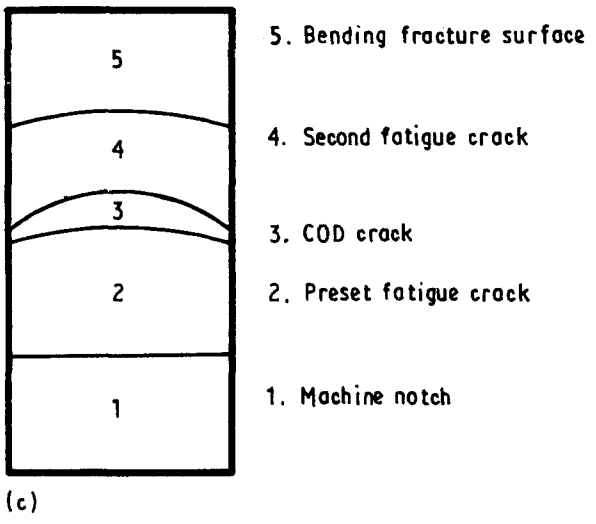

Figure 1 Low-magnification optical fractographs of the COD test samples: (a) top row (from left to right), ingots 6, 5, 4, 3, 2; bottom row, ingot 1; (b) top row (from left to right), ingots 6, 5, 4, 3, 2; bottom row, ingot 1; (c) schematic illustration of COD specimen fracture surface.

are larger than those in Fig. 1a. In Fig. 1a and b, each of the COD test samples had a machine notch (area 1), a preset fatigue crack (area 2), a COD crack (area 3), a second fatigue crack (area 4), and finally a bending crack fracture surface (area 5): this is illustrated schematically in Fig. 1c.

From the COD crack and bending fracture surfaces it is readily seen that there is tearing of the banded microstructure (i.e. there are some secondary cracks, a type of lamellar tear which formed perpendicular to the crack propagation through the specimen). This is because there are some elongated MnS inclusions present at the interfaces between the bands of pearlite and the proeutectoid ferrite in the hot-rolled steel sheet. Those inclusions are in the form of a thin film.

The SEM fractography of the tensile specimens is shown in Fig. 2a–f, corresponding to the specimens from ingots 6–1. In addition to the typical ductile "cup-and-cone" fracture, there is a banded structure fracture for all six samples, and the tearing crack from the elongated MnS inclusions (Fig. 2a and c) in the specimens from ingots 6 and 4 without a RE treatment.

4. Discussion

The SEM observations, Fig. 2, only show a banded structure with some lamellar tearing along the banded structure in the fracture surface for the untreated (ingot 6) and calcium-only treated (ingot 4) specimens. All other samples showed a typical ductile fracture of the banded structure. These fractographic observations were in agreement with the previous microstructural observations [4] that there are elongated MnS inclusions in ingots 6 and 4, but none of these inclusions in the RE-treated ingots, because of effective inclusion shape control, i.e. MnS inclusions are replaced by the spherical RES (rare-earth sulphide) inclusions which can retain their spherical shape during hot rolling. The formation of the secondary cracks may also be due to the very different mechanical properties of the pearlite and proeutectoid ferrite. This probably happened in the case of bending fracture, as seen in Fig. 1.

The fracture pattern of the tensile specimens can be described using a brittle–ductile composite model, as shown schematically in Fig. 3. The 16 Mn steel has a banded structure of alternate pearlite and proeutectoid ferrite constituents [4]. In this banded structure, the pearlite is the brittle constituent, and the proeutectoid ferrite is the ductile constituent; see Table IV for typical mechanical properties of pearlite and ferrite [6]. The ductile fracture of the banded proeutectoid ferrite–pearlite structure proceeds as follows. Voids in the pearlite regions nucleate the normal ductile cusps, and the fractures show the pearlitic fracture at the base of the ductile dimples [7, 8]. In the pearlite regions, dimples are formed which are coalesced voids (see Fig. 2). The voids are first formed in the pearlite regions and/or the inclusion–matrix interfaces. The consequent growth and coalescence of micro-voids leads to final fracture in plain carbon steels [9].

The strength and hardness of pearlite is higher than that of ferrite, whereas elongation and reduction of area for pearlite is less than that for ferrite. When both of the constituents experience a tensile stress, Fig. 3a, the stress partitioning results in a stress enhancement in the pearlite due to its "hard" nature with respect to ferrite. Microcracks will then be formed in pearlite at

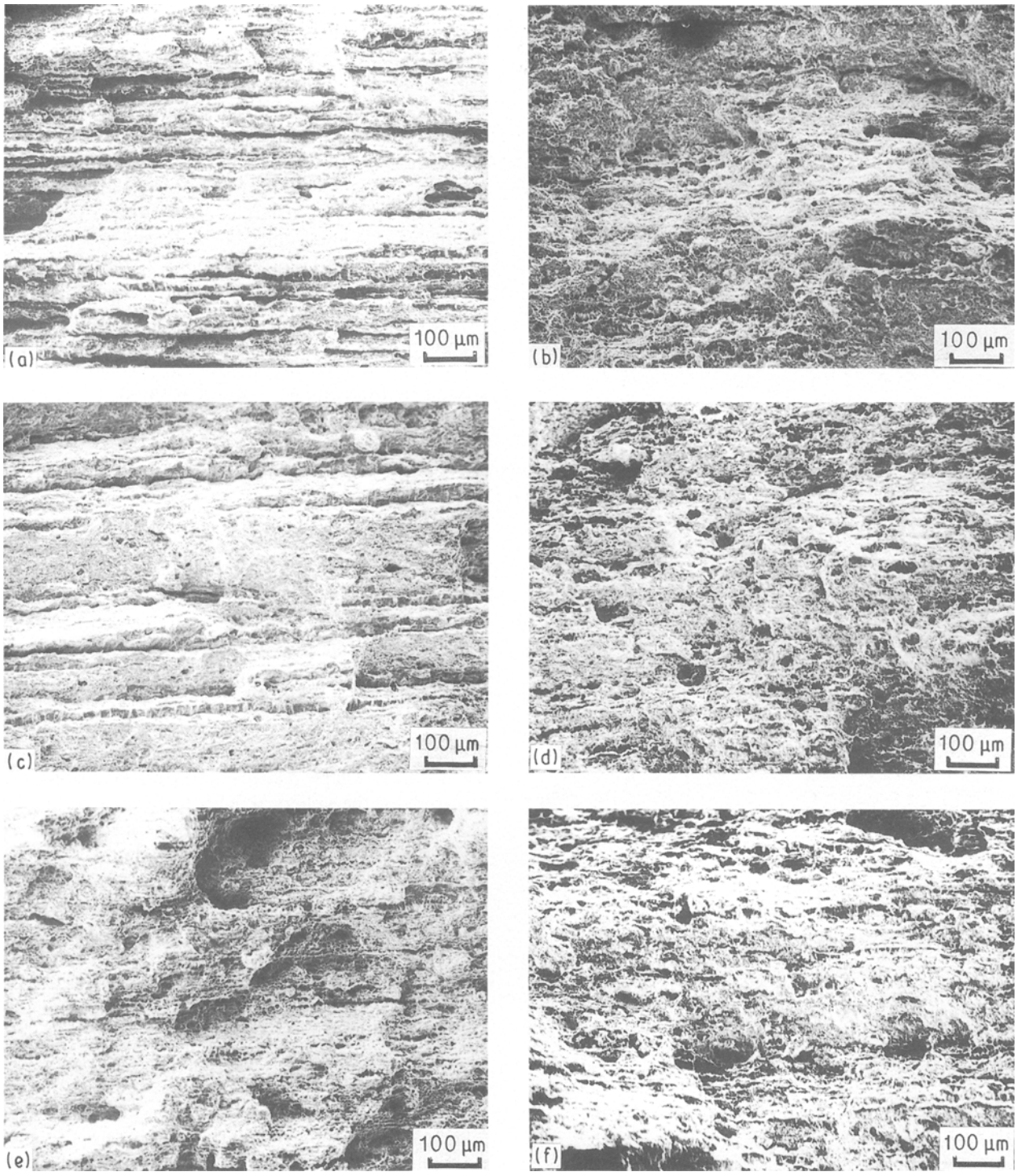

Figure 2 Typical SEM fractographs of tensile fracture surfaces at room temperature. (a) Ingot 6, (b) ingot 5, (c) ingot 4, (d) ingot 3, (e) ingot 2 and (f) ingot 1.

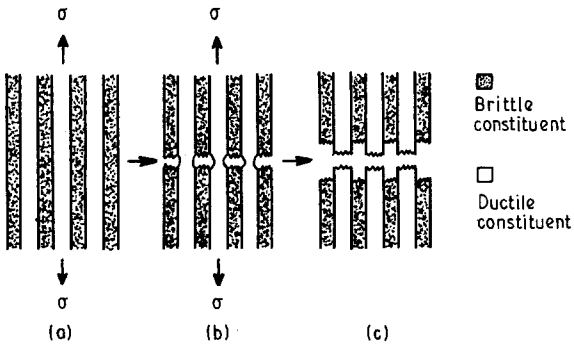

Figure 3 A schematic representation of the fracture processes for a banded brittle (pearlite)–ductile (ferrite) microstructure.

either the Fe_3C/α-Fe or the inclusion/matrix interfaces. The proeutectoid ferrite will continue to deform in a ductile manner without microcracks, Fig. 3b, and the final ductile fracture of the proeutectoid ferrite leaves "extrusions" on the fracture surface, Fig. 3c. Such extrusions were observed by fractography, Fig. 2, in our samples.

The "composite" nature of the microstructure of the steel can also be shown by their tensile properties listed in Table III, and the properties of pearlite and ferrite (Table IV) [6]. By applying the rules for mechanical equilibrium of composites [10]

$$\sigma = V_p\sigma_p + V_f\sigma_f \quad (1)$$

TABLE IV The typical mechanical properties of pearlite and ferrite [6]

Constituents	Tensile strength, σ_t (MPa)	Yield strength, σ_y (MPa)	Brinell hardness, HB	Elongation, δ (%)	Reduction of area, ψ (%)
Ferrite	210	136	96	40	75
Pearlite	980	588	240	10	14

where σ, σ_p and σ_f are strengths of the steel, the pearlite constituent and the proeutectoid ferrite, respectively, and V_p and V_f are the volume fractions of pearlite and proeutectoid ferrite constituents, respectively. Using the yield strength and the hardness in Tables III and IV, a value of $V_f = 0.66$ was obtained. Optical metallography gave a similar value for V_f on an area basis (a grid system was used for the V_f measurement). A value for V_f can also be obtained using the lever law. The alloying elements, both manganese and silicon decrease the carbon content of the eutectoid. If the influence of elements manganese and silicon are taken into account, then V_f is about 0.70.

5. Conclusions

Studies of a 16 Mn steel in the hot-rolled condition have shown that RE treatments can improve the fracture properties in the transverse direction of the sheet. This fracture property improvement is due to the inclusion shape control with a RE treatment. The inclusion shape control modifies elongated MnS inclusions into spherical RE sulphide inclusions in the hot-rolling condition, and thereby reduces the stress concentration at the inclusions. However, all the treatments gave the same room-temperature tensile properties (less than 10% difference). A "composite" model is proposed to describe the fracture behaviour. For the application of this model both SEM fractography and a tensile test are required.

Acknowledgements

One of the authors (L.S.) is grateful to Professor J. Chen, Institute of Metal Research, Academia Sinica, Shenyang, People's Republic of China for his supervision of this work. The steel was provided by the Anshan Iron and Steel Corporation, Anshan, People's Republic of China. Continued financial support to L. Shi is being provided by the Natural Sciences and Engineering Research Council of Canada through an Operating Grant (A4391) awarded to Professor D. O. Northwood.

References

1. E. OROWAN, in "Internal Stress and Fatigue in Metals", edited by G. M. Rassweiler and W. L. Grube (Elsevier, Amsterdam, 1959) p. 59.
2. C. E. SIMS, *Trans. Met. Soc. AIME* **215** (1959) 382.
3. L. A. LUYCKX, in "Industrial Application of Rare Earth Elements", edited by K. A. Gschneidner Jr (American Chemical Society, Washington, DC, 1981) p. 43.
4. L. SHI, J. CHEN and D. O. NORTHWOOD, *J. Mater. Engng* **13**, (1991) 273.
5. *Idem., J. Mater. Engng. Performance* **1** (1992) 21.
6. D. S. CLARK and W. R. VARNEY, "Physical Metallurgy for Engineers", 2nd Edn (Van Nostrand Princeton, NJ, 1962) p. 128.
7. A. GANGULEE and J. GURLAND, *Trans. Met. Soc. AIME* **239** (1967) 269.
8. T. GLADMEN, B. HOLMES and I. D. McIVOR, "Effect of Second Phase Particles on the Mechanical Properties of Steel" (The Iron and Steel Institute, London, 1971) p. 68.
9. L. E. MILLER and G. C. SMITH, *J. Iron Steel Inst.* **208** (1970) 998.
10. W. D. NIX, J. C. GIBELING and D. A. HUGHES, *Metall. Trans.* **16A** (1985) 2215.

Received 17 June
and accepted 16 December 1991